

Some Recent Advances and Remaining Questions Regarding Unimolecular Rate Theory

WILLIAM L. HASE

Department of Chemistry Wayne State University,
Detroit, Michigan 48202

Received January 13, 1998

Introduction

Unimolecular reactions are important for many different chemical processes, e.g., atmospheric and combustion chemistry,¹ peptide fragmentation,² and the dissociation of clusters,^{3,4} and it is important to have accurate theoretical models for unimolecular dynamics and kinetics. A widely used model for calculating unimolecular rate constants at fixed energy E and angular momentum J is the Rice–Ramsperger–Kassel–Marcus (RRKM) theory,^{5,6} which assumes a transition state for passing from reactants to products and rapid intramolecular vibrational energy redistribution (IVR) among the degrees of freedom of the dissociating molecule. As a result of this rapid IVR, a microcanonical ensemble of states is maintained during the unimolecular decomposition. The RRKM rate constant for E and J is

$$k(E, J) = \frac{N^\ddagger(E, J)}{h\rho(E, J)} \quad (1)$$

where $N^\ddagger(E, J)$ is the transition state's sum of states and $\rho(E, J)$ the unimolecular reactant's density of states. RRKM theory is viewed as a statistical theory since the rate constant is calculated from statistical mechanical properties and an understanding of the actual dissociation dynamics is unnecessary.

Anharmonicity and vibrational/rotational coupling must be treated correctly to accurately evaluate $N^\ddagger(E, J)$ and $\rho(E, J)$ in eq 1. Recent studies⁷ have shown that anharmonic effects become very important for fluxional molecules, such as clusters and macromolecules, with multiple potential energy minima as shown in Figure 1. A harmonic RRKM model, based on the deepest potential energy minimum, is seriously in error for highly fluxional molecules.⁷

The sum and densities of states in eq 1 are calculated for the active degrees of freedom, for which IVR is rapid. Within the framework of RRKM theory, there is the

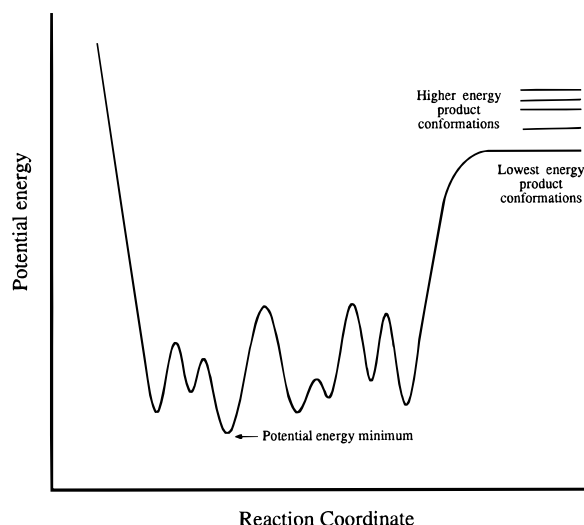


FIGURE 1. A model reaction coordinate potential energy curve for a fluxional molecule. Reprinted with permission from ref 7. Copyright 1996 American Institute of Physics.

possibility that some modes are not active, but are adiabatic and stay in fixed quantum states \mathbf{n} during the reaction.⁸ For this situation, eq 1 becomes

$$k(E, J, \mathbf{n}) = \frac{N^\ddagger(E, J, \mathbf{n})}{h\rho(E, J, \mathbf{n})} \quad (2)$$

In addition to affecting the number of active degrees of freedom, the fixed \mathbf{n} also affects the threshold $E_0(\mathbf{n})$ for dissociation. The degree of freedom which has received considerable interest, regarding its activity or adiabaticity, is the one associated with the K rotational quantum number.^{9–11} With extensive vibrational/rotational coupling K will be active, but with weak coupling an adiabatic treatment will be more accurate.

The prediction of RRKM theory is that $k(E)$ increases with increasing E . At low energies, where $N^\ddagger(E, J)$ is small, there are measurable incremental increases in $N^\ddagger(E, J)$ and steps in $k(E, J)$ are observed.^{12,13} If the density of states of the reactant molecule is sufficiently small, unimolecular dissociation occurs via isolated or overlapping compound state resonances.^{14,15} The rate constants for these resonances may vary by orders of magnitude within a narrow energy interval, $E \rightarrow E + \Delta E$.^{16–19} This elementary decay at the level of individual resonance quantum states has been connected to statistical unimolecular decay.^{20,21} The average rate constant for these statistical resonance states, within the interval $E \rightarrow E + \Delta E$, is thought to be well-approximated by the RRKM $k(E)$.²⁰

In most experimental studies of unimolecular dissociation the energy resolution is not sufficient to excite an individual resonance state, and instead a superposition of states is prepared, which often localizes the energy within a subset of the molecule's degrees of freedom.⁶ With rapid IVR this initial localized state will evolve into a microcanonical ensemble so that, except for the shortest times, the unimolecular decomposition will appear to be RRKM.²² Experimental and theoretical studies have sug-

William L. Hase received a B.S. degree in chemistry from the University of Missouri, Columbia, in 1967 and a Ph.D. in physical chemistry from New Mexico State University in 1970. He then carried out postdoctoral studies at the University of California, Irvine, before joining the faculty at Wayne State University. Under the tutelage of his Ph.D. and postdoctoral advisors, John W. Simons and Don L. Bunker, he developed his life-long interest in unimolecular reaction dynamics.

gested that IVR may not compete with unimolecular decomposition for unimolecular reactions with shallow potential energy wells.^{23,24} The lifetime for the unimolecular reactant is much shorter than the time for IVR, and the result is non-RRKM kinetics. This type of behavior may be important for numerous chemical reactions and has been implicated for S_N2 ion-molecule complexes^{23,25-27} and for the trimethylene biradical intermediate in cyclopropane isomerization.^{24,28,29}

The above advances and remaining questions, concerning unimolecular rate theory, are reviewed in this Account. Examples are given of how including anharmonicity for fluxional molecules and treating the K quantum number as adiabatic or active affects RRKM unimolecular rate constants. A brief discussion, including examples, is given of the way in which the statistical state specific decomposition of quantum resonance states affects thermal unimolecular rate constants. The final discussion concerns the likely prevalence of non-RRKM kinetics for unimolecular reactions with shallow potential energy wells.

RRKM Unimolecular Rate Theory

Anharmonic Effects for Fluxional Molecules. Extensive applications of RRKM theory have been made to unimolecular reactions, for which there is a single potential energy minimum for the reactant molecule.^{5,6} For such reactions, harmonic sums and densities of state are usually used to calculate the $k_h(E,J)$ harmonic approximation to the actual anharmonic RRKM rate constant in eq 1. These two rate constants are related by

$$k_{\text{anh}}(E,J) = k_h(E,J)/f_{\text{anh}}(E,J) \quad (3)$$

where $f_{\text{anh}}(E,J)$ is the anharmonic correction factor.³⁰ For most RRKM calculations $f_{\text{anh}}(E,J)$ is assumed to be unity. However, recent experimental measurements of state densities indicate it may be as high as 10 for unimolecular reactants with a single potential energy minimum.¹⁷

Anharmonic corrections are expected to be very important for highly fluxional molecules such as clusters and macromolecules.⁷ Figure 1 illustrates a possible potential energy curve for a fluxional molecule. There are multiple minima (i.e., conformations) separated by barriers much lower than that for dissociation. Thus, a moderately excited fluxional molecule may undergo rapid transitions between its many conformations, and all will contribute to the molecule's unimolecular rate constant. Many different conformations are expected for the products, but near the dissociation threshold E_0 , only one set of product conformations is accessible. As the energy is increased, thresholds for other product conformations are reached. For energies near E_0 , there is very little excess energy in the transition state and the harmonic approximation should be very good for the transition state's sum of states. Thus, for $E \approx E_0$ the anharmonic correction in eq 3 primarily results from anharmonicity in the reactant density of states and is given by $f_{\text{anh}}(E,J) = \rho_{\text{anh}}(E,J)/\rho_h(E,J)$.

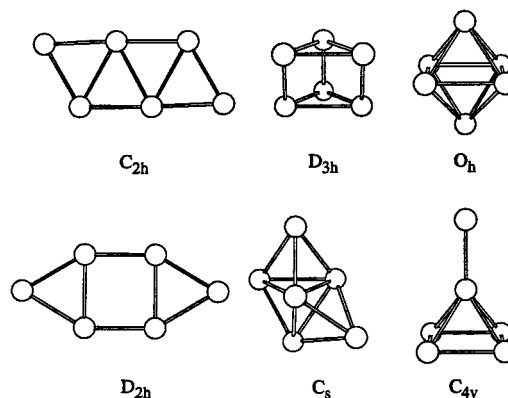


FIGURE 2. Potential energy minima for Al_6 . The unimolecular thresholds for the C_{2h} , D_{3h} , C_s , O_h , C_{4v} , and D_{2h} minima are 43.8, 40.0, 39.6, 38.8, 31.4, and 20.9 kcal/mol, respectively.

In general, determining the quantum mechanical $f_{\text{anh}}(E,J)$ requires knowing the anharmonic quantum mechanical energy levels for both the reactant and transition state. Obtaining this information is even formidable for small molecules with only one potential energy minimum and is impractical for large fluxional molecules with multiple minima. Classical mechanics may be used to estimate the importance of anharmonicity, and various approaches may be used to calculate classical anharmonic sums and densities of state. Relative densities of states versus energy may be determined by fixed temperature molecular dynamics simulations.^{7,31} They are then converted into actual densities by solving the classical phase integral⁷ or using adiabatic switching^{7,31,32} to determine the actual density for at least one energy.

There is a caveat in using the above approaches to calculate densities of states for fluxional molecules. Because of their multiple minima, there is an ambiguity in choosing a symmetry number to correct for the number of equivalent potential energy wells, since the number of equivalent wells varies for the different minima.⁷ On the other hand, it is straightforward to compare the classical anharmonic RRKM rate constant^{6,33} and the standard classical harmonic one based on the deepest potential energy minimum. The former may be calculated from classical trajectories by following the initial decay of a microcanonical ensemble of states for the unimolecular reactant. Such a calculation has been performed for dissociation of the Al_6 cluster,⁷ using a model analytic potential energy function written as a sum of Lennard-Jones and Axilrod-Teller potentials. Structures of some of the Al_6 minima, for this potential function, are shown in Figure 2. The deepest potential minimum has C_{2h} symmetry and a classical $\text{Al}_6 \rightarrow \text{Al}_5 + \text{Al}$ dissociation energy E_0 of 43.8 kcal/mol. For energies 30–80 kcal/mol in excess of this E_0 , the value of f_{anh} determined from the trajectories varies from 200 to 130. (The harmonic RRKM rate constants are calculated for a reaction path degeneracy of 6.) As discussed above, even larger corrections are expected at lower energies,³⁴ particularly for $E \approx E_0$. For the bigger cluster Al_{13} , the anharmonic correction varies from 5500 to 1200 for excess energies in the range of 85–185 kcal/mol. These calculations illustrate that, to cal-

culate accurate RRKM unimolecular rate constants for fluxional molecules, it is of critical importance to include anharmonic corrections.

The K Quantum Number: Adiabatic or Active. There is considerable uncertainty in how angular momentum should be treated in RRKM calculations.^{9–11} Though the quantum number J representing the total angular momentum is a constant of the motion, the proper treatment of the K quantum number, the projection of J onto the molecular symmetry axis, is less certain. Coriolis coupling can mix the $2J + 1K$ levels for a particular J and destroy K as a good quantum number. For this situation K is considered an *active* degree of freedom. On the other hand, if the coriolis coupling is weak, the K quantum number may retain its integrity and it may be possible to measure the unimolecular rate constant as a function of K as well as of E and J . For this case, K is an *adiabatic* degree of freedom. Thus, in addition to anharmonicity corrections, another remaining issue in RRKM unimolecular rate theory is the extent of vibrational/rotational coupling.

It is straightforward to introduce active and adiabatic treatments of K into the widely used RRKM model which represents vibrational and rotational degrees of freedom as harmonic oscillators and rigid rotors, respectively.⁹ If K is adiabatic, a molecule containing total vibrational rotational energy E , and in a particular J, K level, has a vibrational density of states $\rho[E - E_r(J, K)]$, where $E_r(J, K)$ is the rotational energy. Similarly, the transition state's sum of states for the same E, J , and K is $N^\ddagger[E - E_0 - E_r^\ddagger(J, K)]$, where E_0 is the unimolecular threshold. The RRKM rate constant for the K adiabatic model is

$$k(E, J, K) = \frac{N^\ddagger[E - E_0 - E_r^\ddagger(J, K)]}{h\rho[E - E_r(J, K)]} \quad (4)$$

Mixing of the $2J + 1K$ levels, for the K active model, results in the following sums and densities of states:

$$\rho(E, J) = \sum_{K=-J}^J \rho[E - E_r(J, K)] \quad (5)$$

$$N^\ddagger(E, J) = \sum_{K=-J}^J N^\ddagger[E - E_0 - E_r^\ddagger(J, K)] \quad (6)$$

The RRKM rate constant for the K active model is then

$$k(E, J) = \frac{\sum_{K=-J}^J N^\ddagger[E - E_0 - E_r^\ddagger(J, K)]}{h \sum_{K=-J}^J \rho[E - E_r(J, K)]} \quad (7)$$

In these models the treatment of K is the same for the molecule and transition state. It is worthwhile noting that *mixed mode RRKM models* are possible in which K is treated differently in the molecule and transition state.⁹

Calculations have been performed to compare the above RRKM models for $k(E, J)$ and $k(E, J, K)$.⁹ As expected,

the sensitivity of $k(E, J, K)$ to K tends to depend on the transition state's sum of states instead of the reactant's density of states, since the rotational energy is a larger fraction of the transition state's total energy. There are some J, K levels for which $E_r^\ddagger(J, K)$ is greater than $E - E_0$, and thus, the unimolecular dissociation channel is closed. For prolate and oblate tops this occurs at high and low K , respectively. Similarly, whether $k(E, J, K)$ decreases or increases with an increase in K depends on the transition state structure, i.e., a prolate or oblate top.

The difference in Lindemann–Hinshelwood thermal unimolecular rate constants $k_{\text{uni}}(\omega, T)$, calculated with the above active and adiabatic models for K , is most pronounced at the $\omega \rightarrow 0$ low-pressure limit.⁹ If the variational criterion⁶ is unimportant for choosing the transition state structure, the high-pressure limiting rate constant is the same for the K active and adiabatic models. The K adiabatic model gives a lower high-pressure rate constant if the variational criterion is important.

At low pressure $k_{\text{uni}}(\omega, T)$ is proportional to the effective collision frequency multiplied by the density of molecular states which can undergo unimolecular reaction. This density is smaller with K adiabatic in the transition state than with K active. As discussed above, with K adiabatic, there are molecular states for which $E_r^\ddagger(J, K)$ is greater than $E - E_0$ and there are no available states at the transition state through which reaction can occur. As a result the K adiabatic model has a smaller density of reactive molecular states, and it requires a larger effective collision frequency to fit experimental measurements of $k_{\text{uni}}(\omega, T)$ at low pressure.

These K adiabatic and active models have been used in RRKM calculations of $k_{\text{uni}}(\omega, T)$ for $\text{C}_2\text{H}_2\text{Cl} \rightarrow \text{Cl} + \text{C}_2\text{H}_2$ dissociation at low pressure. To fit experimental values of $k_{\text{uni}}(\omega, T)$, the collision frequency is written as $\omega = \beta_c \omega_{\text{LJ}}$, where β_c is the collision efficiency^{35,36} and ω_{LJ} the Lennard-Jones collision frequency. For temperatures in the range of 252–370 K, the fitted β_c values were found to range from 1.6 to 2.4 times larger for models with K adiabatic versus K active in the transition state.⁹ These calculations illustrate the interplay between parameters of RRKM models in fitting rate constants and point out that, until the proper model for K is determined, it will not be possible to deduce physically meaningful collision efficiencies from thermal unimolecular rate constants.

Statistical State Specific Decomposition. Small molecules and larger molecules at lower levels of excitation decompose via isolated compound state (i.e., Feshbach) resonances, which may be viewed as the extension of bound states into the dissociative continuum.^{14–19} Since these resonances are spectrally isolated, they have individual state specific rate constants. Mode specific characteristics may be associated with these rate constants, if it is possible to assign quantum numbers to their resonance states.³⁷ Another limiting case arises when the resonances are unassignable and, with orthogonality constraints maintained, are simply random projections onto any basis set. As a result there are random fluctua-

tions in the rate constants, which has been identified as *statistical state specific* unimolecular decomposition.³⁷

A model for the distribution of statistical state specific rate constants in the energy interval $E \rightarrow E + dE$ is known from work in nuclear physics.³⁸ It is a χ^2 distribution and given by²⁰

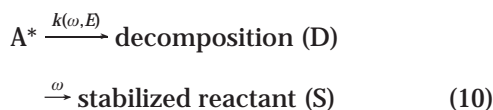
$$P_E(k) = \Gamma\left(\frac{\nu}{2}\right)^{-1} \left(\frac{\nu}{2\bar{k}}\right) \left(\frac{\nu k}{2\bar{k}}\right)^{(\nu/2)-1} \exp\left(-\frac{\nu k}{2\bar{k}}\right) \quad (8)$$

where \bar{k} is the average state specific rate constant

$$\bar{k} = \int_0^\infty kP(k) dk \quad (9)$$

and ν is the “effective number of decay channels”. For large ν , $P_E(k)$ approaches a delta function peaked around \bar{k} . Thus, there are no fluctuations in the state specific rate constants and exponential decay within the energy interval $E \rightarrow E + dE$ results, as predicted by RRKM theory. It has been argued²⁰ that \bar{k} should approximate the RRKM rate constant $k(E)$ and, for energies above the unimolecular threshold E_0 , ν equals the transition state sum of states $N^\ddagger(E)$. For energies below E_0 , ν is related to the tunneling probability.²⁰ In addition to eq 8, a more general distribution function has been advanced for $P_E(k)$.^{20,21}

It is of interest to identify the effects of the above microscopic statistical state specificity on macroscopic unimolecular kinetics. The gas-phase unimolecular decomposition of a monoenergetically excited molecule A^* , in a collision environment, is often interpreted by the mechanism³⁹



For standard RRKM theory, there is only one rate constant at energy E and $k(\omega, E)$ in the above mechanism is independent of ω .⁴⁰ However, for statistical state specific decomposition, $k(\omega, E)$ is pressure dependent.⁴¹ Resonance states with large rate constants are more likely to contribute to dissociation at high pressures, while all states contribute equally at low pressures. This effect is seen in standard RRKM theory when a molecule is not excited at a fixed energy, but with a distribution of energies.³⁹

When $P_E(k)$ in eq 8 is incorporated into the above mechanism, it is found that $k(\omega, E)$ has very simple forms in the high-pressure $\omega \rightarrow \infty$ and low-pressure $\omega \rightarrow 0$ limits.⁴¹ For the $\omega \rightarrow \infty$ limit, $k(\omega, E)$ is independent of ν and equals \bar{k} . At the $\omega \rightarrow 0$ limit, $k(\omega, E)$ depends on the value of ν . It equals zero for ν of 1 and 2, and equals $[(\nu - 2)/\nu]\bar{k}$ for $\nu > 2$ and finite. The latter value is the same as the value of k for the maximum in the $P(k)$ distribution when $\nu > 2$ and finite. Thus, the pressure dependence of $k(\omega, E)$ becomes negligible as ν becomes large.

It has been found that the 28 300 cm^{-1} photodissociation of H_2CO occurs via statistical state specific resonances, whose rate constants are represented by a $P_E(k)$ distribution with $\nu = 4$.²⁰ For this case $k(\omega, E)$ varies from

\bar{k} to $\bar{k}/2$ between the $\omega \rightarrow \infty$ and $\omega \rightarrow 0$ limits. Thus, in very low-pressure experimental conditions the monoenergetic rate constant is predicted to be a factor of 2 smaller than the RRKM prediction.

If there are fluctuations, e.g., given by $P_E(k)$ in eq 8, the Lindemann–Hinshelwood monoenergetic unimolecular rate constant $k_{\text{uni}}(\omega, E)$ may be expressed as^{40,42}

$$k_{\text{uni}}(\omega, E) = \int_0^\infty dk P_E(k) \frac{k\omega}{k + \omega} \quad (11)$$

Averaging over E gives the Lindemann–Hinshelwood thermal unimolecular rate constant³⁷

$$k_{\text{uni}}(\omega, T) = \frac{1}{Q} \int_0^\infty dE e^{-E/k_B T} \rho(E) k_{\text{uni}}(\omega, E) \quad (12)$$

where Q is the reactant’s partition function.

Equations 11 and 12 show that a distribution of state specific rate constants only affects $k_{\text{uni}}(\omega, T)$ at intermediate pressures, where $k_{\text{uni}}(\omega, T)$ is lowered by including $P_E(k)$.⁴¹ In the second-order low-pressure limit, $k_{\text{uni}}(\omega, T)$ is proportional to ω and the Boltzmann-weighted density of states of reacting molecules. At high pressures it is only the average rate constant \bar{k} for each energy interval which contributes to $k_{\text{uni}}(\omega, T)$.

To study how statistical state specificity affects thermal unimolecular rate constants, $k_{\text{uni}}(\omega, T)$ curves have been calculated for $\text{HO}_2 \rightarrow \text{H} + \text{O}_2$ dissociation using standard RRKM and RRKM theory with the $P_E(k)$ distribution included,⁴⁰ i.e., eqs 11 and 12. Quantum dynamical calculations by Schinke and co-workers¹⁸ show that HO_2 dissociates via isolated resonances, whose wave functions have random characteristics and whose rate constants appear to be statistical state specific, in accord with the Porter–Thomas $P_E(k)$ distribution. Comparisons were made between $k_{\text{uni}}(\omega, T)$ curves calculated with the $P_E(k)$ distribution and those calculated with standard RRKM theory. The calculations were performed with the rotational quantum number K treated as either active or adiabatic. The maximum difference between the $k_{\text{uni}}(\omega, T)$ curves, calculated with the $P_E(k)$ distribution and by standard RRKM theory, occurs at a higher pressure as the temperature is increased. For the K adiabatic RRKM model, the pressure at which the maximum difference between the two curves occurs smoothly increases from 1×10^4 to 1×10^6 Torr as the temperature is increased from 100 to 6000 K. Figure 3, which gives plots of the maximum difference between the curves as a function of temperature, shows that the sensitivity of the Lindemann–Hinshelwood $k_{\text{uni}}(\omega, T)$ rate constant to the Porter–Thomas $P_E(k)$ distribution depends on whether the K quantum number is treated as active or adiabatic. For example, with K adiabatic the difference between the two curves is 30% at 100 K, while only 5% with K active. Thus, to establish the importance of including the $P_E(k)$ distribution when calculating $k_{\text{uni}}(\omega, T)$, one needs to know whether K is adiabatic or active.

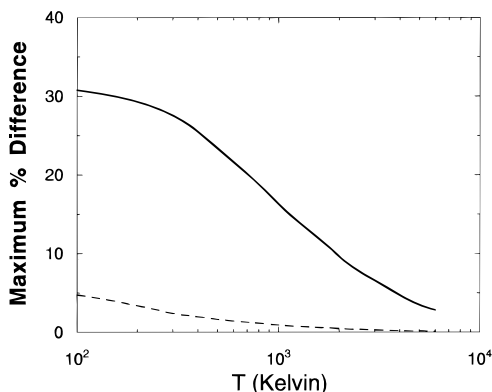
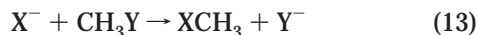


FIGURE 3. Maximum percent difference between $k_{\text{uni}}(\omega, T)$ curves calculated with the Pöter–Thomas $P_E(k)$ distribution and those calculated with standard RRKM theory: (—) K adiabatic model; (---) K active model.

Non-RRKM Kinetics: Effect of Shallow Potential Energy Wells

An assumption widely made in chemical kinetics is that reactions which proceed through potential energy wells form intermediates with rapid IVR and whose unimolecular kinetics is thus in accord with the RRKM theory.⁶ Insight into limitations of this model have come from trajectory simulations, statistical rate theory calculations, and experimental measurements for the $\text{Cl}^- + \text{CH}_3\text{Cl}$,^{43,44} $\text{Cl}^- + \text{CH}_3\text{Br}$,^{25–27} and $\text{F}^- + \text{CH}_3\text{Cl}$ $\text{S}_{\text{N}}2$ reactions⁴⁵ and of the trimethylene biradical.^{28,29}

Potential energy surfaces for $\text{S}_{\text{N}}2$ reactions of the type



are characterized by shallow potential energy wells ~ 10 kcal/mol deep for the $\text{X}^- \cdots \text{CH}_3\text{Y}$ and $\text{XCH}_3\text{Y} \cdots \text{Y}^-$ pre- and postreaction ion–dipole complexes, which are separated by a $[\text{X}^- \cdots \text{CH}_3 \cdots \text{Y}]^-$ central barrier.²³ To form the $\text{X}^- \cdots \text{CH}_3\text{Y}$ prereaction complex, the $\text{X}^- + \text{CH}_3\text{Y}$ relative translational energy E_{rel} must be transferred to CH_3Y vibrational and/or rotational degrees of freedom.⁴³ Trajectories for the $\text{Cl}^- + \text{CH}_3\text{Cl}$ system show the energy transfer is initially to CH_3Cl rotation, which excites the three low-frequency intermolecular modes of the $\text{Cl}^- \cdots \text{CH}_3\text{Cl}$ complex.⁴³ Lifetimes determined for this complex from trajectories and experiments⁴⁶ are reproduced by an RRKM model with only three active degrees of freedom.⁴⁴ Energy transfer to the higher frequency CH_3Cl intramolecular modes, which initiates the $\text{S}_{\text{N}}2$ reaction, occurs on a much longer time scale. The trajectories indicate the bottleneck for energy transfer between the intermolecular and intramolecular modes may trap trajectories in the vicinity of the central barrier, causing extensive barrier recrossings.^{23,47}

As a result of strong coupling between the C–Y stretch mode of CH_3Y and the reaction coordinate in the vicinity of the central barrier, which gives rise to a large reaction path curvature, exciting the C–Y stretch mode opens up a direct mechanism for reaction 13.⁴⁸ This mechanism becomes more important at low CH_3Y rotational energies so that the incoming ion can orient the CH_3Y dipole. Both a direct substitution trajectory and one that forms the

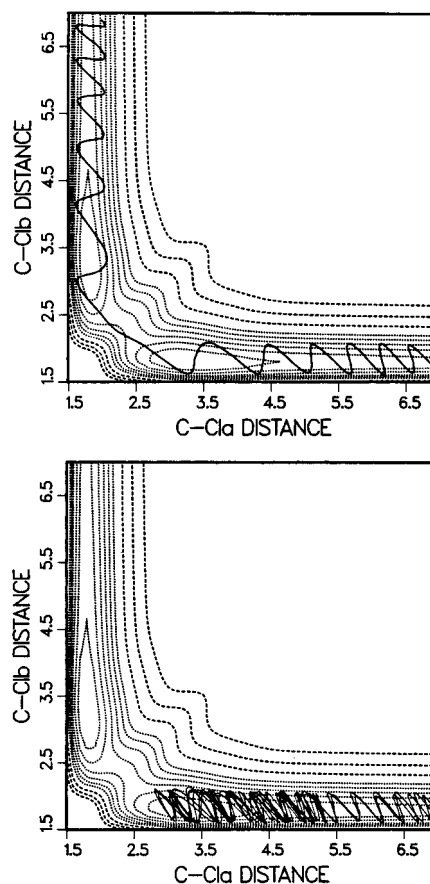


FIGURE 4. $\text{Cl}_a^- + \text{CH}_3\text{Cl}_b$ trajectories which undergo direct substitution and form the $\text{Cl}_a^- \cdots \text{CH}_3\text{Cl}_b$ complex.

prereaction complex are illustrated in Figure 4 for the $\text{Cl}^- + \text{CH}_3\text{Cl}$ system. Direct substitution appears to be only a minor component of the $\text{Cl}^- + \text{CH}_3\text{Cl}$ $\text{S}_{\text{N}}2$ reaction at 300 K.²³

The apparent weak coupling between the low-frequency intermolecular and high-frequency intramolecular modes of the $\text{X}^- \cdots \text{CH}_3\text{Y}$ complex suggests that mode specific unimolecular reaction should be observed when specific modes of the complex are excited. This type of behavior is observed in a trajectory study of $\text{Cl}^- \cdots \text{CH}_3\text{Br}$ decomposition.²⁶ Crossing the central barrier and forming the $\text{ClCH}_3 + \text{Br}^-$ product are promoted by exciting the intramolecular modes, particularly the C–Br stretch, while exciting the intermolecular modes promotes $\text{Cl}^- + \text{CH}_3\text{Br}$ formation. The exact details of these mode specific effects are highly sensitive to the potential energy surface.

The non-RRKM dynamics described above is not observed for all $\text{S}_{\text{N}}2$ reactions. The kinetics for the $\text{Cl}^- + \text{ClCH}_2\text{CN}$ $\text{S}_{\text{N}}2$ reaction is well-described by RRKM theory.⁴⁹ Apparently the much deeper well for the $\text{Cl}^- \cdots \text{ClCH}_2\text{CN}$ complex and the lower intramolecular vibrational frequencies for the ClCH_2CN moiety make the time scale for IVR competitive with that for unimolecular decomposition.

Non-RRKM dynamics is also seen in trajectory simulations of the trimethylene biradical $\cdot\text{CH}_2\text{CH}_2\text{CH}_2\cdot$. As shown in Figure 5, this biradical has a very shallow well intermediate between propylene and geometrical isomers

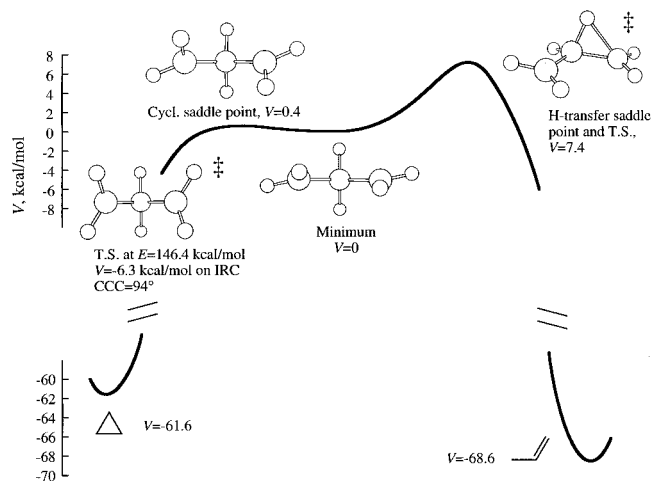


FIGURE 5. Minimum potential energy along the cyclopropane \leftrightarrow trimethylene \leftrightarrow propylene reaction path. Reprinted from ref 50. Copyright 1996 American Chemical Society.

of cyclopropane.⁵⁰ The cyclopropane isomers and trimethylene are interconnected via three different transition states (TSs) each with a different reaction coordinate motion, i.e., con and dis TSs in which the two terminal CH₂ groups undergo conrotatory and disrotatory motion, respectively, and a cis TS in which only one of the terminal CH₂ groups rotates. After the reactive system crosses one of these TSs to form trimethylene, RRKM theory assumes trimethylene does not retain a memory of how it is formed and a statistical model may be used to determine whether trimethylene closes to form cyclopropane via the con, dis, and/or cis TSs. Trajectory calculations of the trimethylene dynamics on a modified AM1 potential energy surface suggest that this model is incomplete.²⁸ Boltzmann distributions of trajectories, directed toward trimethylene, are initialized at each of the three TSs. A strong relationship is found between the TS excited and the TS at which ring closure occurs. Exciting at the con TS yields 65% ring closure via the con TS, while 67% of the ring closure occurs by the cis TS when this TS is excited. Similar types of TS memory in reaction dynamics have been observed in trajectory simulations of other organic intermediates.²⁴

Perspective

From the above discussions, it is clear that unimolecular rate theory remains a fertile and exciting area of research. RRKM rate constant calculations need to become more accurate by including anharmonic corrections and treating vibrational/rotational coupling. No definitive a priori procedures have been established to identify which reactions are not accurately described by RRKM theory. S_N2 ion-dipole complexes and organic biradicals are two important reactive systems which exhibit non-RRKM dynamics.

The author thanks the National Science Foundation for financial support and his students and collaborators who made the research discussed here possible.

References

- (1) Steinfield, J. I.; Francisco, J. S.; Hase, W. L. *Chemical Kinetics and Dynamics*; Prentice Hall: Englewood Cliffs, NJ, 1989; p 496.
- (2) Wysocki, V. H.; Dongre, A. R. In *Large Ions: Their Vaporization, Detection and Structural Analysis*; Baer, T., Powis, I., Ng, C. Y., Eds.; Wiley: New York, 1996; p 145.
- (3) Hales, D. A.; Su, C.-X.; Lian, L.; Armentrout, P. B. *J. Phys. Chem.* **1994**, *100*, 1049.
- (4) López, M. J.; Jellinek, J. *Phys. Rev. A* **1994**, *50*, 1445.
- (5) Gilbert, R. G.; Smith, S. C. *Theory of Unimolecular and Recombination Reactions*; Blackwell: London, 1990.
- (6) Baer, T.; Hase, W. L. *Unimolecular Reaction Dynamics. Theory and Experiment*; Oxford: New York, 1996.
- (7) Peslherbe, G. H.; Hase, W. L. *J. Chem. Phys.* **1996**, *105*, 7432.
- (8) Robinson, P. J.; Holbrook, K. A. *Unimolecular Reactions*; Wiley: New York, 1972; p 67.
- (9) Zhu, L.; Hase, W. L.; Kaiser, E. W. *J. Phys. Chem.* **1993**, *97*, 311.
- (10) North, S. W.; Hall, G. E. *Ber. Bunsen-Ges. Phys. Chem.* **1997**, *101*, 459.
- (11) Grebenshchiko, S. Y.; Flöthmann, H.; Schinke, R.; Bezel, I.; Wittig, C.; Kato, S. *Chem. Phys. Lett.* **1998**, *285*, 410.
- (12) Green, W. H.; Moore, C. B.; Polik, W. F. *Annu. Rev. Phys. Chem.* **1992**, *43*, 591.
- (13) Chatfield, D. C.; Friedman, R. S.; Milke, S. L.; Lynch, G. C.; Allison, T. C.; Truhlar, D. G.; Schwenke, D. W. In *Dynamics of Molecules and Chemical Reaction*; Wyatt, R. E., Zhang, J. Z. H., Eds.; Marcel Dekker: New York, 1996; pp 323–386.
- (14) Mies, F. H. *J. Chem. Phys.* **1969**, *51*, 798.
- (15) Miller, W. H. *Chem. Rev.* **1987**, *87*, 19.
- (16) Miller, R. E. *Science* **1988**, *240*, 447.
- (17) Polik, W. F.; Guyer, D. R.; Moore, C. B. *J. Chem. Phys.* **1990**, *92*, 3453.
- (18) Dobbyn, A. J.; Stumpf, M.; Keller, H.-M.; Schinke, R. *J. Chem. Phys.* **1996**, *104*, 8357.
- (19) Qi, J.; Bowman, J. M. *J. Chem. Phys.* **1996**, *105*, 9884.
- (20) Polik, W. F.; Guyer, D. R.; Miller, W. H.; Moore, C. B. *J. Chem. Phys.* **1990**, *92*, 3471.
- (21) Miller, W. H.; Hernandez, R.; Moore, C. B.; Polik, W. F. *J. Chem. Phys.* **1990**, *93*, 5657.
- (22) Bunker, D. L.; Hase, W. L. *J. Chem. Phys.* **1973**, *59*, 4621.
- (23) Hase, W. L. *Science* **1994**, *266*, 998.
- (24) Carpenter, B. K. *Am. Sci.* **1997**, *85*, 138.
- (25) (a) Viggiano, A. A.; Morris, R. A.; Paschkewitz, J. S.; Paulson, J. F. *J. Am. Chem. Soc.* **1992**, *114*, 10477. (b) Wang, H.; Hase, W. L. *J. Am. Chem. Soc.* **1995**, *117*, 9347.
- (26) Peslherbe, G. H.; Wang, H.; Hase, W. L. *J. Am. Chem. Soc.* **1996**, *118*, 2257.
- (27) Craig, S. L.; Brauman, J. I. *J. Phys. Chem. A* **1997**, *101*, 4745.
- (28) Doubleday, Jr., C.; Bolton, K.; Hase, W. L. *J. Am. Chem. Soc.* **1997**, *119*, 5251.
- (29) Hrovat, D. A.; Fang, S.; Borden, W. T.; Carpenter, B. K. *J. Am. Chem. Soc.* **1997**, *119*, 5253.
- (30) Troe, J. *J. Chem. Phys.* **1977**, *66*, 4758.
- (31) Weerasinghe, S.; Amar, F. G. *J. Chem. Phys.* **1993**, *90*, 4967.
- (32) Reinhardt, W. P. *J. Mol. Struct.* **1990**, *223*, 157.
- (33) Shalashilin, D. V.; Thompson, D. L. *J. Phys. Chem. A* **1997**, *101*, 961.

- (34) Because of the size of Al_6 and its long unimolecular lifetime, it becomes impractical to simulate the classical dissociation of Al_6 for energies in excess of E_0 much smaller than 30 kcal/mol.
- (35) Tardy, D. C.; Rabinovitch, B. C. *Chem. Rev.* **1977**, *77*, 369.
- (36) Troe, J. J. *J. Chem. Phys.* **1977**, *66*, 4745.
- (37) Hase, W. L.; Cho, S.-W.; Lu, D.-H.; Swamy, K. N. *Chem. Phys.* **1989**, *139*, 1.
- (38) Porter, C. E.; Thomas, R. G. *Phys. Rev.* **1956**, *104*, 483.
- (39) Rabinovitch, B. S.; Setser, D. W. *Adv. Photochem.* **1964**, *3*, 1.
- (40) To simplify the presentation, summations over J and K are not included in the rate constant expressions presented in this section. The complete expressions can be found in Song, K.; Hase, W. L. *J. Phys. Chem.* **1998**, *102A*, 1292.
- (41) Lu, D.-H.; Hase, W. L. *J. Phys. Chem.* **1989**, *93*, 1681.
- (42) Miller, W. H. *J. Phys. Chem.* **1988**, *92*, 4261.
- (43) Hase, W. L.; Cho, Y. J. *J. Chem. Phys.* **1993**, *98*, 8626.
- (44) Peslherbe, G. H.; Wang, H.; Hase, W. L. *J. Chem. Phys.* **1995**, *102*, 5626.
- (45) (a) Su, T.; Morris, R. A.; Viggiano, A. A.; Paulson, J. F. *J. Phys. Chem.* **1990**, *94*, 8426. (b) O'Hair, R. A. J.; Davico, G. E.; Hacaloglu, H.; Dang, T. T.; DePuy, C. H.; Bierbaum, V. M. *J. Am. Chem. Soc.* **1994**, *116*, 3609. (c) Wang, H.; Hase, W. L. *J. Am. Chem. Soc.* **1997**, *119*, 3093.
- (46) Li, C.; Ross, P.; Szulejko, J. E.; McMahon, T. B. *J. Am. Chem. Soc.* **1996**, *118*, 9360.
- (47) Truhlar, D. G.; Garrett, B. C.; Klippenstein, S. J. *J. Phys. Chem.* **1996**, *100*, 12771.
- (48) Wang, H.; Hase, W. L. *Chem. Phys.* **1996**, *212*, 247.
- (49) Viggiano, A. A.; Morris, R. A.; Su, T.; Wladkowski, B. D.; Craig, S. L.; Zhong, M.; Brauman, J. I. *J. Am. Chem. Soc.* **1994**, *116*, 2213.
- (50) Doubleday, C., Jr.; Bolton, K.; Peslherbe, G. H.; Hase, W. L. *J. Am. Chem. Soc.* **1996**, *118*, 9922.

AR970156C